Journal of Medicinal and Nanomaterials Chemistry 1 (2022) 159-173

SPC

Journal of Medicinal and Nanomaterials Chemistry

Journal homepage: https://jmnc.samipubco.com/

Original Research Article

Synthesis, characterization and catalytic activity of zinc oxide nanoparticles functionalized with metallo-thoiosemicarbazones

Varun Kumar Bale, Hussain Reddy Katreddi*

Department of Chemistry, Sri Krishnadevaraya University, Anantapuramu-515003, (A.P.) India

ARTICLE INFORMATION

Received: 29 April 2022
Received in revised: 13 May 2022
Accepted: 14 May 2022
Available online: 26 May 2022

DOI: 10.48309/JMNC.2022.2.7

KEYWORDS

Zinc oxide nanoparticles
Metallo-Thiosemicarbazones
Functionalization
4-Nitrophenol
4-Aminophenol

ABSTRACT

We report zinc oxide nanoparticles functionalized with metallo-thoiosemicarbazones for the first time. The objective of the present work is to report the synthesis, characterization and catalytic activity of novel zinc oxide nanoparticles (ZnONPs) functionalized with copper(II) and palladium(II) complexes of 4-hydroxybenzaldehyde thiosemicarbazone (BTSC) ligand. In the present study, as-synthesized ZnONPs and itspost-functionalized ZnONPs@Cu-BTSC and ZnONPs@Pd-BTSC were prepared and analyzed using UV-visible and FT-IR, PXRD, and SEM-EDX techniques. The X-ray diffraction pattern of ZnONPs showed intense peaks indexed to (1 0 0), (0 0 2), (1 0 1), (1 0 2), (1 1 0), (1 0 3) and (1 1 2) planes which corresponded to hexagonal wurtzite phase of zinc oxide (ZnO) nanoparticles. The catalytic activity of ZnONPs, ZnONPs@Cu-BTSC, and ZnONPs@Pd-BTSC in reducing 4-nitrophenol was investigated. The ZnONPs@Pd-BTSC showed higher catalytic activity compared with that of the ZnONPs@Cu-BTSC.

Corresponding author, email: khussainreddy@yahoo.co.in (H.R. Katreddi).

Graphical Abstract

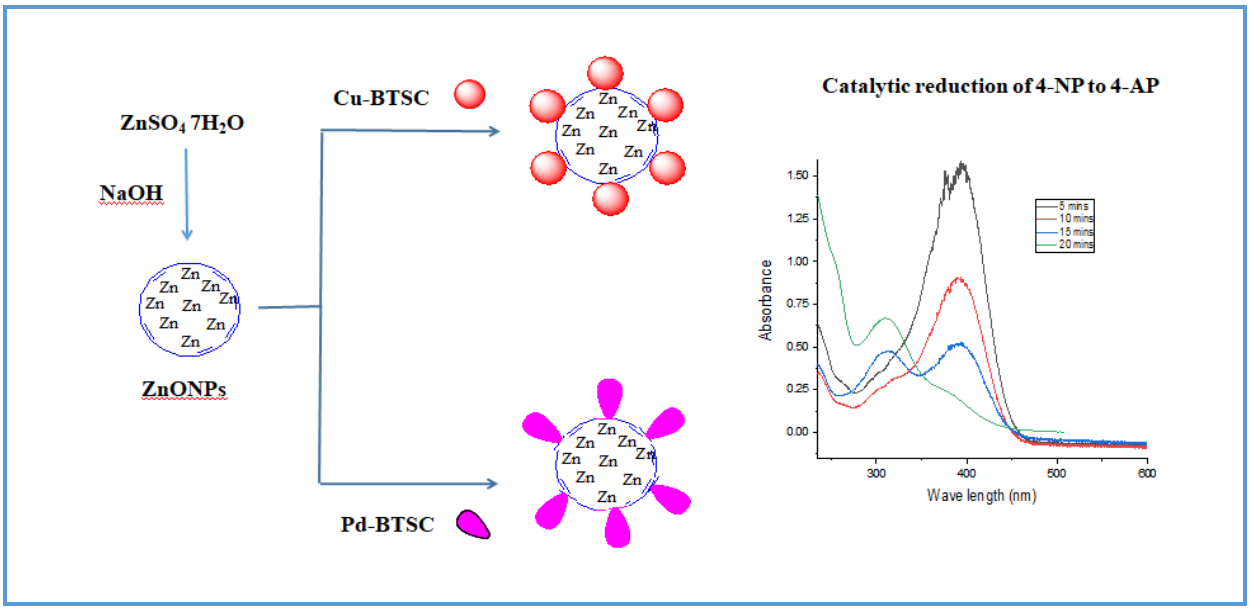

Introduction

Metal nanoparticles (MNPs) have displayed conspicuous catalytic activity at very low concentrations due to their unique chemical and physical features [1] and high surface area to volume ratio. The nano-sized MNPs are stable even at high temperatures and pressure [2]. Zinc oxide nanoparticles (ZnONPs) displayed interesting chemical, electronic and optical properties. Zinc is an essential trace metal for living organisms, including human beings. The presence of zinc is indispensable in many enzymes [3] and without which the enzymes become inactive. Due to the non-toxic nature and essentiality of zinc in living organisms zinc oxide nanoparticles are regarded as heartening materials for pharmaceutical products.

The zinc oxide nanoparticles (ZnONPs) are of interest due to their usage in the manufacture of many industrial products [4–6], such as memory devices, photoconductive material, LED, transistors, solar cells, cosmetics, and catalysts. ZnONPs have been synthesized using co-precipitation [7], hydrothermal [8] techniques, and by using leaf/plant extracts [9, 10]. Recently ZnO nanoparticles were used as photocatalysts in the degradation of dyes [11], antibacterial agents [9, 10], and as nanocomposites for lubricating oil [12]. In addition, ZnONPs exhibited interesting optical properties [13]. Further, these are non-toxic, non-corrosive, and do not produce harmful side products. ZnO nanoparticles have been used as catalysts in several organic reactions [14–19] due to their environmentally friendly features.

Several attempts were made to modify zinc oxide nanoparticles to develop more efficient catalysts in organic synthesis. Commercial ZnONPs were coated [20] by APTES under different conditions. The coated nano particles were analyzed using PXRD, BET, TEM, and SEM techniques. Ramasamy *et al.* [21] have investigated the purpose of surface alteration of ZnONPs and their toxic effecton fibroblast cells. Synthesis of tripodal catecholate and their anchoring on ZnONPs were reported [22] recently. In another attempt [23], these nanoparticles were coated with ϒ-aminopropyltriethoxysilane and investigated their photocatalytic activity. Khan *et al.* [24]

reported catalytic applications of ZnONPs functionalized with polymer microgels. Recently, spherical ZnO was modified [25] with Ag nanoparticles and investigated their catalytic and antibacterial activities.

Attempts were made to prepare bimetallic MNPs due to their broad applications. Wang *et al.* [26] have investigated ZnO-Ag composite photocatalysts. Pandiyan *et al.* [27] have reported antibacterial and anticancer activity of Ag-Au/ZnO nanostructures. Improved biomedical properties were observed for bi-metal nanoparticles. It is interesting to functionalize ZnONPs with coordination compounds to develop new hybrid catalysts. Therefore, it is considered worthwhile to synthesize, characterize, and investigate the catalytic activity of as-synthesized ZnONPs and novel post-functionalized ZnONPs with copper and palladium complexes of 4-hydroxybenzaldehyde thiosemicarbazone (BTSC) in the reduction toxic pollutant 4-nitrophenol (NP) [28] to functional 4-aminophenol (AP) [29, 30]. The reduction of 4-NP to 4-AP has been considered an interesting research activity as the former is the most toxic water pollutant. In contrast, the latter has several applications such as corrosion inhibitors, antioxidant and photographic developer. The catalytic activity of present metallo-thoiosemicarbazone functionalized zinc oxide nanoparticles is delineated in this research article.

Experimental

Materials and methods

The metal salts, chemicals, and solvents used were of AR grade. Thiosemicarbzide and 4-hydroxybenzaldehyde were used to prepare 4-hydroxybenzaldehyde thiosemicarbazone (BTSC). Copper(II) chloride dihydrate [$CuCl_2.2H_2O$] and palladium chloride [$PdCl_2$] were used in the preparation of complexes of BTSC. Ethanol (C_2H_5OH) was distilled before use.

Synthesis of zinc oxide nanoparticles

Zinc sulfate (0.2 M) solution was prepared by dissolving 2.87 g of $ZnSO_4.7H_2O$ in 50 mL of de-ionized water taken in a 250 mL beaker. The solution was heated to about 80 °C on a hot plate and added 50 mL 2 M NaOH dropwise with constant stirring and heated for 30 min. The contents were chilled to room temperature(RT). A white substance formed was gathered by filtration, washed with hot water, and dried in a vacuum. The white substance was ground and heated at 120 °C in an electric air oven for about 6 h to obtain ZnO nanoparticles (ZnONPs). The yield was 70%.

Synthesis of 4-hydroxybenzaldedhyde thiosemicarbazone (BTSC)

A 5 g of 4-hydroxybenzaldehyde was taken 100 mL round bottom flask and dissolved in 10 mL of methanol. Then hot aqueous solution (20 mL) of thiosemicarbazide (3.75 g) was added drop-wise and heated under reflux for 30 min. A yellow colored crystalline substance was formed at the bottom of the flask. It was acquired by filtration washed with hot water and methanol, and then dried in air. Yield: 74%, Melting point: 216-218 °C. Schematic for the synthesis of BTSC ligand is shown in Scheme 1.

Spectral characterization of BTSC

IR (KBr) (ν_{max}/cm^{-1}): 3494, 3496, 3376, 3360, 3130, 1609, and 1164; ^1H NMR (number MHz, solvent): δ 9.88 (s, 1H O-H); 7.83 (s, 1H, C-H), 7.59-7.61 (d, 2H, Ar-H) (J = 8.5 Hz), 6.76-6.78 (d, 2H, J = 8.5 Hz, Ar-H), 8.07 (s, 2H, NH_2), 11.25 (s, 1H, N-H). Mass spectra (m/z), an intense peak was observed at 196 which corresponded to (M+H).

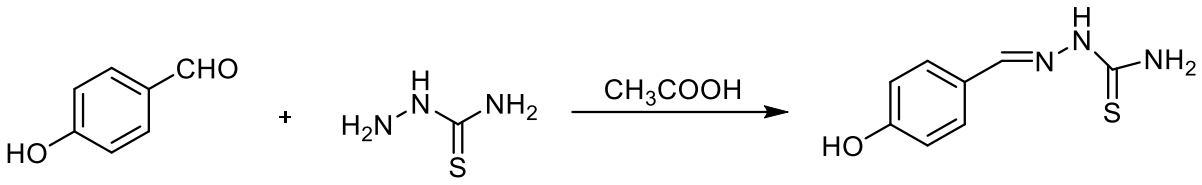

Scheme 1. Synthesis of 4-hydroxybenzaldedhyde thiosemicarbazone (BTSC)

Synthesis of Cu-BTSC complex

A 2 g of BTSC ligand was taken in a 100 mL round bottom flask and dissolved in 20 mL of methanol. Then copper chloride (1.71 g of $CuCl_2.2H_2O$ dissolved in 20 mL methanol) solution was added dropwise to the contents of the round bottom flask and was heated under reflux for 2 h. The contents were cooled to room temperature. Greenish brown colored solid was formed at the bottom of the flask. It was collected by filtration, washed with methanol, and dried. Yield: 64%, IR (KBr) (ν_{max}/cm^{-1}): 3130, 1589, and 1160. Mass spectra: A strong peak appeared at m/z 453.10 in the copper complex's mass spectrum (Figure S1, Supporting Information) corresponding to the formula $Cu(BTSC)_2$.

Synthesis of Pd-BTSC complex

A 2 g of BTSC ligand was taken in a 100 mL round bottom flask and dissolved in 20 mL of methanol. Then palladium chloride (1.42 g of $PdCl_2$ dissolved in 25 mL of 1:5 HCl:methanol) solution was added dropwise to the contents of the round bottom flask and heated under reflux for 1 h. On cooling theflask's contents, dark reddish-brown colored compound was formed. It was acquired by filtration, washed with methanol, and dried. Yield: 67%, IR (KBr) (ν_{max}/cm^{-1}): 3174, 1585, 1135, Mass spectra: A strong peak appeared at m/z 371.78 in mass spectrum (Figure S2, Supporting Information) of palladium complex corresponded to the formula, $Pd(BTSC)Cl_2$.

Synthesis of ZnONPs@Cu-BTSC and ZnONPs@Pd-BTSC

About 0.5 g metal complex (Cu-BTSC or Pd-BTSC) was taken in a 100 mL RB flask and dissolved in 20 mL of ethanol. Then a suspension of ZnONPs (0.4 g in 20 mL of methanol) was added slowly to the contents of the RB flask and heated for 1 h. The contents were cooled, and the solid material was gathered by filtration, washed with methanol, and dried to obtain post- functionalized nanoparticles.

Characterization techniques

Our recently published article described the equipment used to characterize complexes and nanoparticles [31].

Catalytic activity experiments

In the reduction of 4-nitrophenol (4-NP) to 4-aminophenol (4-AP) by sodium borohydride ($NaBH_4$), ZnONPs, ZnONPs@Cu-BTSC, and ZnONPs@Pd-BTSC were used as catalysts. Freshly prepared $NaBH_4$ (1 mL of 0.2 M) and 4-nitrophenol (1.9 mL, 0.2 mM) solutions were taken in a 3 mL quartz cuvette and thoroughly mixed, and the spectrum was recorded immediately in the range of 200-800 nm. The spectra were taken at uniform time intervals (5 min) after the addition and thorough mixing of 0.10 mL of 1% suspension of ZnONPs@Cu-BTSC or ZnONPs@Pd-BTSC in CH_3OH.

Results and Discussion

In continuation of our investigations [32] on the use of nanocatalysts in organic reactions, herein, we synthesized new catalysts ZnONPs@Cu-BTSC or ZnONPs@Pd-BTSC in which the complexes were supported on ZnONPs to uncover their catalytic features in the reduction of 4-nitro phenol (NP) to 4-aminophenol (AP).

FT-IR spectral analysis

Infrared spectra of ZnONPs, (Figure 1) ZnONPs@Cu-BTSC (Figure 2), and ZnONPs@Pd-BTSC (Figure 3) were recorded in KBr discs. IR spectra of ZnONPs@Cu-BTSC and ZnONPs@Pd-BTSC showed peaks at 1605, 1630 cm^{-1} (υ C=N), 1166, 1162 cm^{-1} (υ C=S), 603, 626 cm^{-1} (υ Zn-O) respectively which indicated the binding complexes to the as-synthesized zinc nanoparticles.

Powder X-ray diffraction studies

Diffractograms of as-synthesized ZnONPs and post functionalized ZnONPs@Cu-BTSC and ZnONPs@Pd-BTSC were recorded at 2θ of 20-80°. The XRD patterns of standard ZnO (JCPDS-36-1451), ZnONPs, ZnONPs@Cu-BTSC, and ZnONPs@Pd-BTSC are depicted in Figure 4.

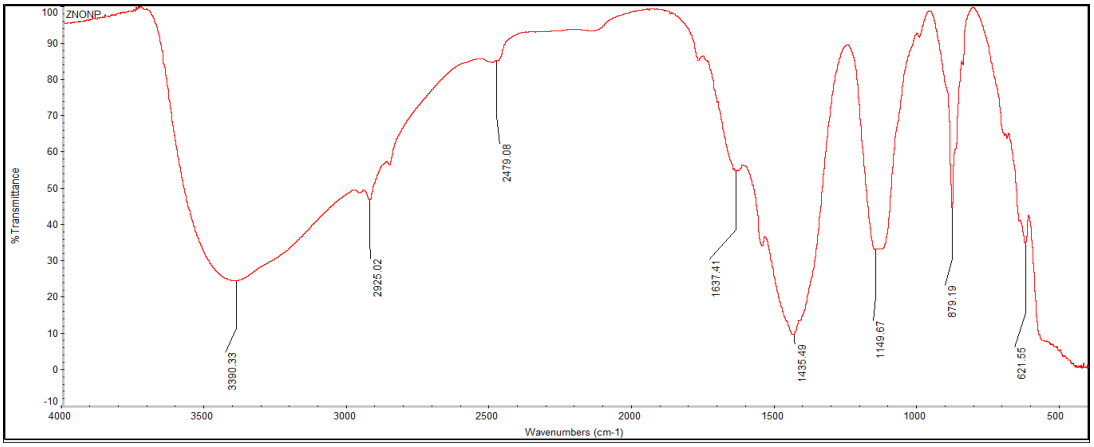

Figure 1. IR spectrum of ZnONPs

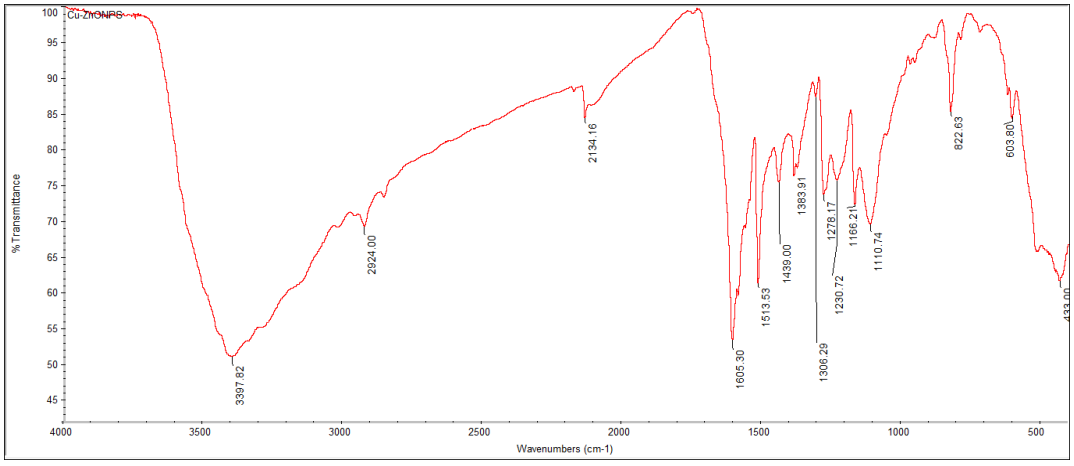

Figure 2. IR spectrum of ZnONPs@Cu-BTSC

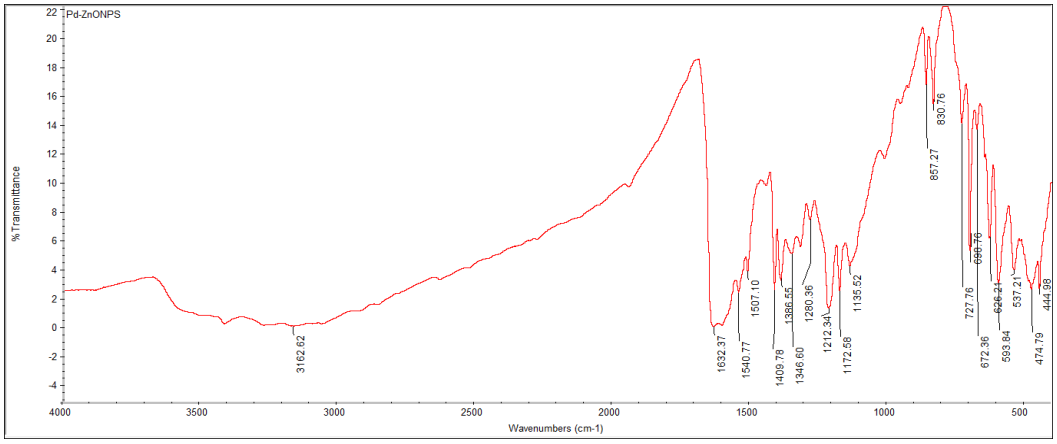

Figure 3. IR spectrum of ZnONPs @Pd -BTSC

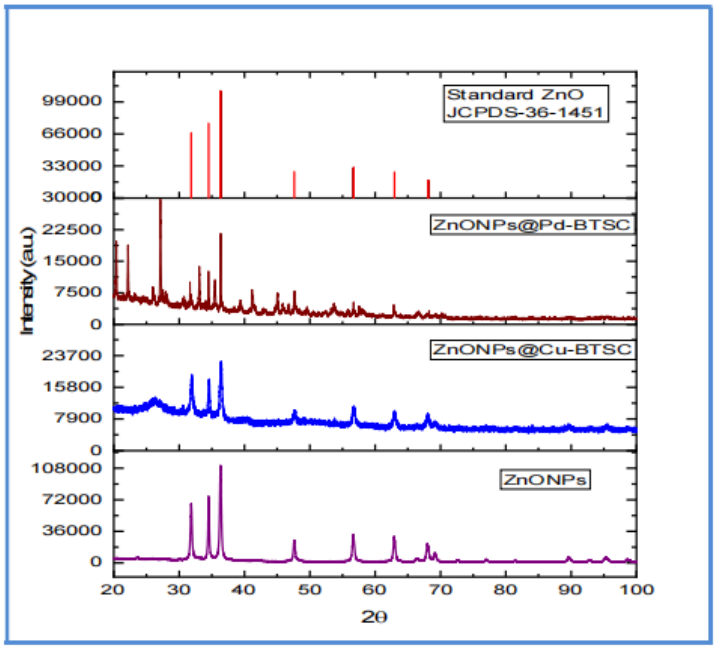

Figure 4. XRD patterns of Standard ZnO(JCPDS-36-1451), native ZnONPs, ZnONPs@Cu-BTSC, and ZnONPs@Pd-BTSC

The X-ray diffraction pattern of as-synthesized ZnONPs showed intense peaks at 31.83, 34.48, 36.31, 47.56, 56.63, 62.89, 67.97 which could be indexed to (1 0 0), (0 0 2), (1 0 1), (1 0 2), (1 1 0), (1 0 3) and (1 1 2) respectively which corresponded to hexagonal wurtzite phase of zinc oxide (ZnO) nanoparticles. The peaks observed in spectra of ZnONPs coincided with Standard ZnO (JCPDS-36-1451). ZnONPs@Cu-BTSC and ZnONPs@Pd-BTSC also exhibited similar peaks as observed in the spectra of as-synthesized ZnONPs. The experimental data with diffraction angles of standard ZnOJCPDS-36-1451 is presented in Table 1.

Particle size calculation

The average particle size of metal nanoparticles as calculated using the well-known Debye-Scherer formula [33–35]. The particle size of the as-synthesized ZnONPs (30-50 nm) was less than post-functionalized ZnONPs@Cu-BTSC (35-70 nm) and ZnONPs@Pd-BTSC (40-80 nm).

Scanning electron microscopy(SEM) and energy dispersive X-ray spectroscopy (SEM-EDX) studies

The surface morphology and grain size of present zinc nanoparticles were examined using the SEM technique. The micrographs of ZnONPs, ZnONPs@Cu-BTSC, and ZnONPs@Pd-BTSC are shown in Figure 5.

The SEM micrographs revealed particle size and morphology changes between native ZnONPs and ZnONPs@Cu-BTSC/ZnONPs@Pd-BTSC. The difference in morphology and particle size between native ZnONPs and ZnONPs@Cu-BTSC/ZnONPs@Pd-BTSC indicated the successful post-functionalization of as-synthesized ZnONPs with metal complexes. SEM's grain size data are similar (Table 2) to particle size obtained from PXRD analysis. The results indicated that the metal complexes were effective in controlling the grain size of zinc nanoparticles.

EDX analysis revealed the elemental composition of newly synthesized zinc nanoparticles. The spectrum of ZnONPs is shown in Figure 6. It confirmed the presence of zinc and oxygen. The weight percentages of elements are given in Table 3. The peak at 0.5 keV is related to the binding energy of oxygen (OKα), and the peak at 0.27 is assigned to carbon (CKα). The peaks at 1.02, 8.63 and 9.51 keV are assigned to zinc (ZnL_1), (ZnKa), and (ZnKb), respectively.

The EDX spectrum of ZnONPs@Cu-BTSC is shown in Figure 7. It confirmed the presence of zinc, copper, carbon, oxygen, nitrogen, and sulfur in significant quantities. The elemental data are given in Table 3. The peaks at 0.5, 0.78, 0.27 keV are related to the binding energy of oxygen (OKα), nitrogen (NKa), and carbon (CKα), respectively. The peaks at 2.34 and 2.48 are assigned to sulfur (SKa and SKb), and peaks at 2.67 and 2.91 correspond to chlorine (Cl Ka and Cl Kb). The peaks at 0.84, 0.94, 8.04, and 8.94 keV are allocated to CuL1, CuKa, and CuKb, respectively. The peaks at 1.02, 8.63and 9.51 keV are specified to zinc (ZnL_1), (ZnKa), and (ZnKb), respectively.

The EDX spectrum of ZnONPs@Pd-BTSC is shown in Figure 8. It indicated the presence of zinc, palladium, carbon, oxygen, nitrogen and sulfur in major quantities. The elemental data are included in Table 3.

Table 1. Diffraction peaks and peak indexing of standard ZnO (JCPDS-36-1451) and ZnONPs, ZnONPs@Cu-BTSC and ZnONPs@Pd-BTSC

2 θ (diffraction peaks) and Peak indexing				
Standard ZnO JCPDS-36-1451	ZnONPs	ZnONPs@Cu-BTSC	ZnONPs@Pd-BTSC	(h k l)
31.84	31.83	31.93	31.68	1 0 0
34.52	34.48	34.57	34.50	0 0 2
36.33	36.31	36.38	36.36	1 0 1
47.63	47.56	47.76	47.66	1 0 2
5671	56.63	56.66	56.71	1 1 0
62.96	62.89	62.95	62.85	1 0 3
68.13	67.97	68.10	68.24	1 1 2

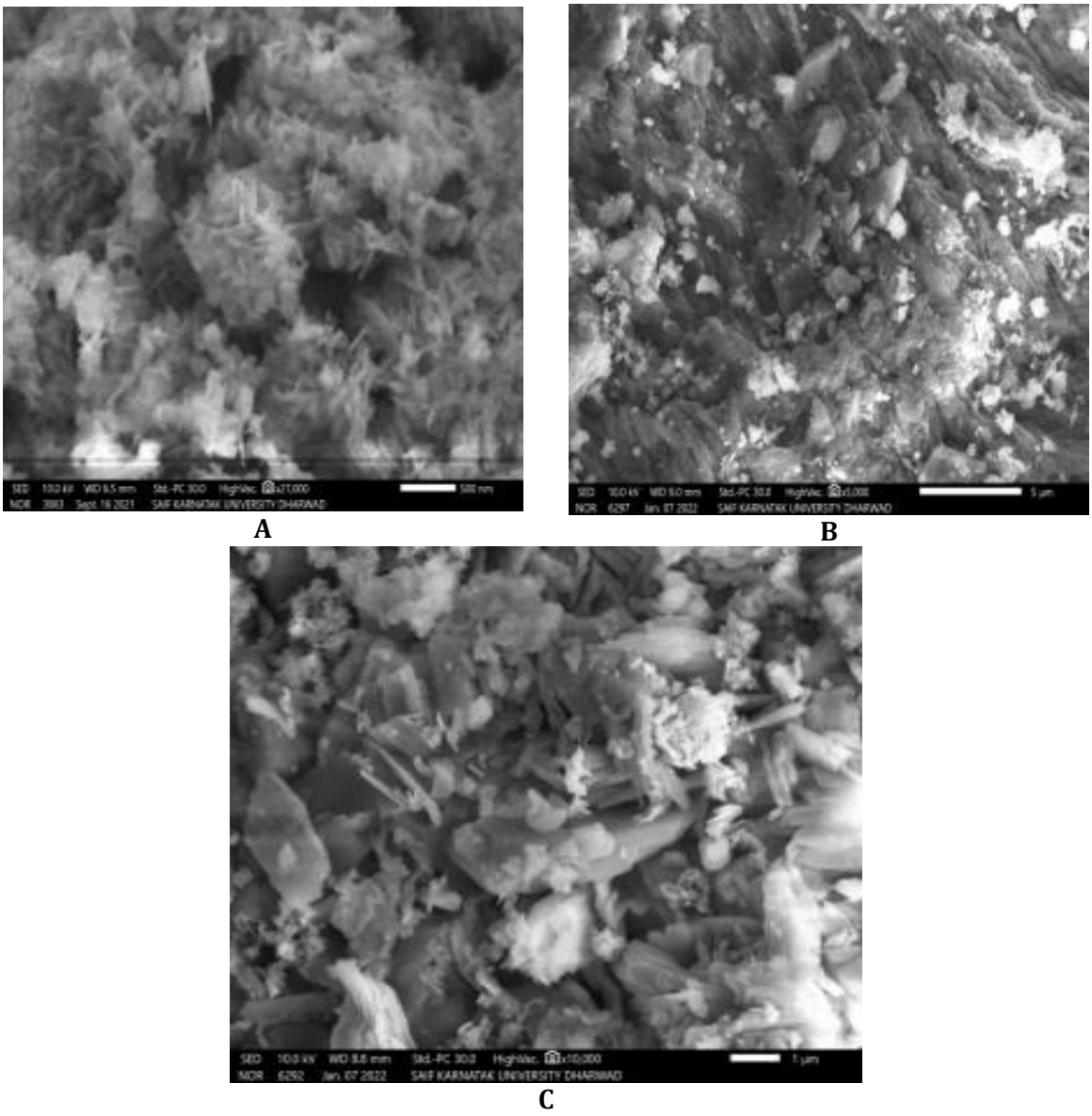

Figure 5. SEM micrographs of (A) ZnONPs, (B) ZnONPs@Cu-BTSC and (C) ZnONPs@Pd-BTSC

Table 2. Comparison of particle size (nm) data of zinc nanoparticles form PXRD and SEM

Nanoparticle	PXRD	SEM
ZnONPs	30-50 nm	45-60 nm
ZnONPs@Cu-BTSC	35-70 nm	50-80 nm
ZnONPs@Pd-BTSC	40-80 nm	50-85 nm

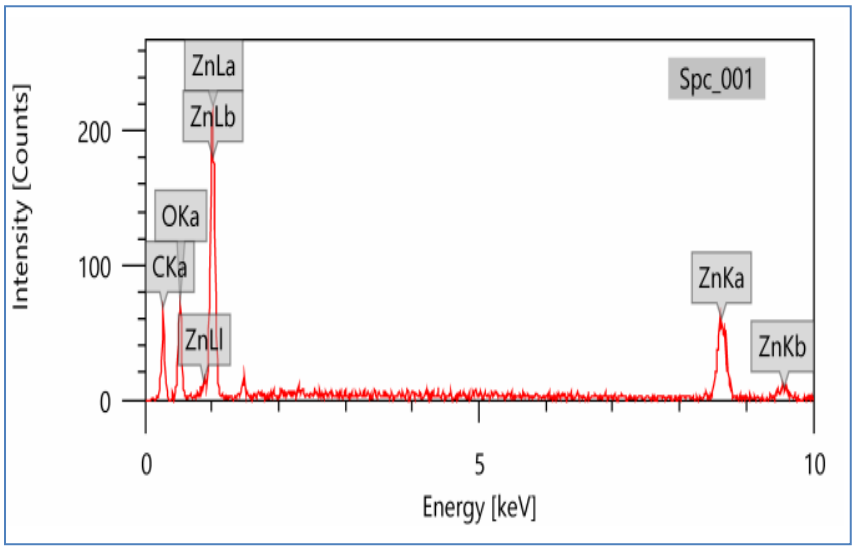

Figure 6. EDX spectrum of ZnONPs

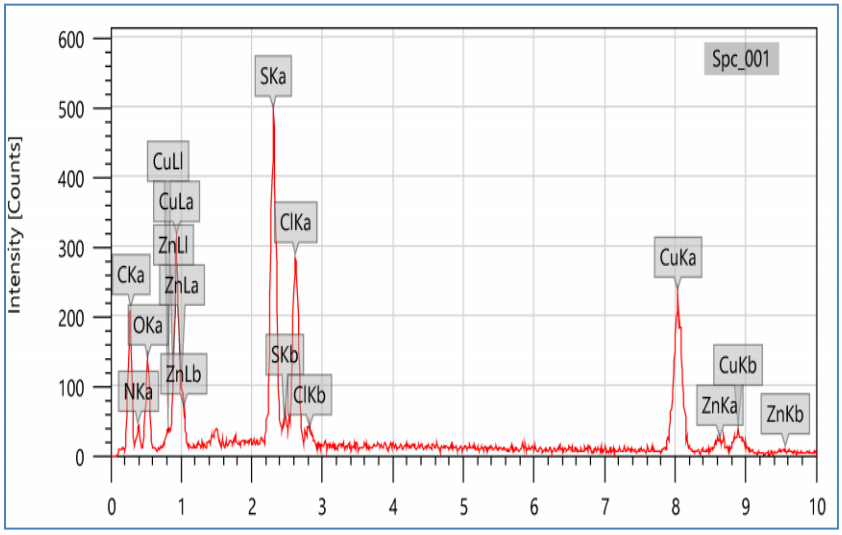

Figure 7. EDX spectrum of ZnONPs@Cu-BTSC

Table 3. Elemental composition of ZnONP from EDX spectrum

Element line	ZnONPs		ZnONPs@Cu-BTSC		ZnONPs@Pd-BTSC	
	Mass %	Atom %	Mass %	Atom %	Mass %	Atom %
C (K)	29.93	54.37	19.55	38.46	12.11	29.24
N (K)	-	-	7.01	12.27	7.70	15.95
O (K)	21.59	29.45	12.70	15.65	12.60	22.84
S (K)	-	-	8.01	4.92	4.54	4.11
Cl (K)	-	-	5.47	3.04	5.97	4.89
Cu (K)	-	-	12.01	8.68	-	-
Pd (K)	-	-	-	-	13.81	3.77
Zn (K)	48.48	16.18	35.25	16.98	43.27	19.21

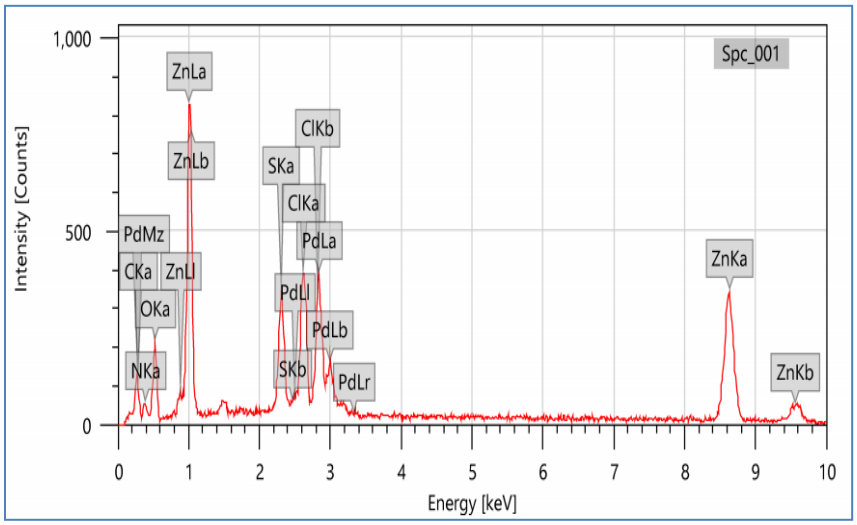

Figure 8. EDX spectrum of ZnONPs@Pd-BTSC

The peaks at 0.5, 0.78, and 0.27 keV are related to the binding energy of oxygen (OKa), nitrogen (NKa), and Carbon (CKa), respectively. The peaks at 2.34 and 2.48 corresponded to sulfur (SKa & SKb), and peaks at 2.67 and 2.91 related to chlorine (Cl Ka and Cl Kb). The crests at 2.83 keV are assigned to palladium (L1, La, Lb, and Lr). The peaks at 1.02, 8.63, and 9.51 keV are assigned to zinc (ZnL_1), (ZnKa), and (ZnKb), respectively.

Catalytic activity

UV-visible spectra of 4-nitrophenol in the presence and in the absence of $NaBH_4$ are shown in Figure 9. It showed maximum absorbance (λ_{max}) at 317 nm in the absence of $NaBH_4$. But in the presence of $NaBH_4$, the λ_{max} was shifted to a higher wavelength (400 nm).

Features of 4-NP reduction

The UV–Vis spectrum of the 4-NP in water is shown in Figure 10. It showed a peak at 317 nm. After adding $NaBH_4$, the peak was shifted to 400 nm, indicating the formation of 4-nitrophenolate. The spectrum remained unchanged for a couple of days before adding zinc nanoparticles (catalyst). However, after the addition of ZnONPs the yellow color intensity was decreased. The decoloration was monitored spectrophotometrically with time. The successive decrease in the peak intensity and appearance of a new peak around 300 nm indicated the reduction of 4-NP and formation of 4-AP. The reduction mechanism (Figure S3, Supporting Information) was given before [32].

After adding 0.10 mL of 1% ZnONPs suspension (in methanol), to the cuvette containing reaction mixture (4-NP+$NaBH_4$), spectra were recorded at uniform time intervals. The spectra demonstrated a decrease in the peak intensity at 400 nm with time and the appearance of a new peak around 300 nm after 30 min time interval due to the reduction of 4-NP and formation of 4-AP. In the case of ZnONPs@Cu-BTSC a new peak is observed around 300 nm just at 25 minutes (Figure 11).

In the case of ZnONPs@Pd-BTSC a new peak is more vividly observed around 300 nm just at 20 min (Figure 12). Experimental observations clearly indicated that ZnONPs@Pd-BTSC catalyzes the reduction of 4-NP to 4-AP more rapidly than did with ZnONPs@Cu-BTSC and ZnONPs.

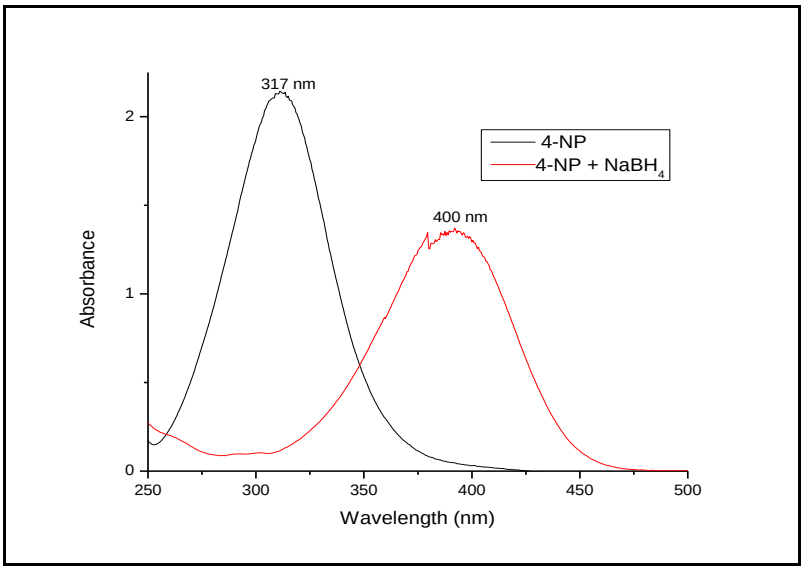

Figure 9. Absorption spectra of 4-nitrophenol (4-NP) and 4-NP + $NaBH_4$

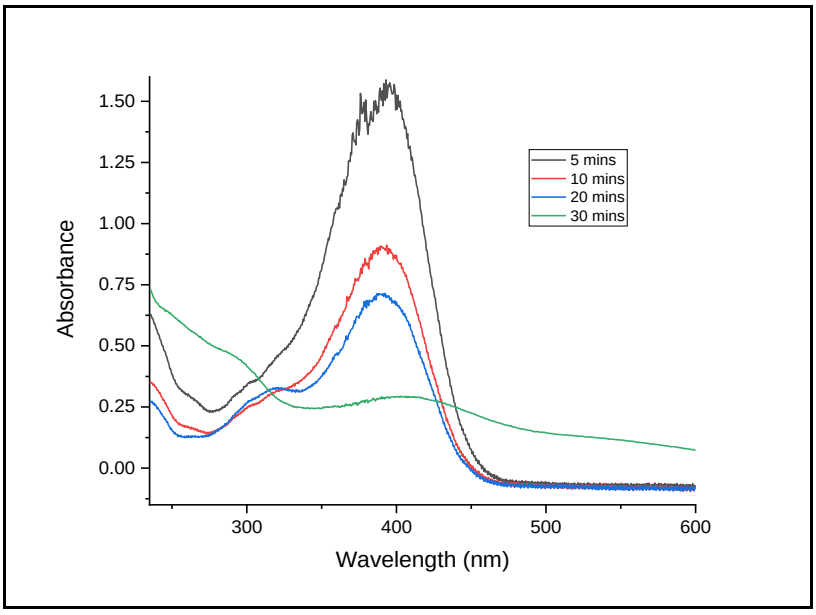

Figure 10. Absorption spectra of reaction mixture containing 4-NP, $NaBH_4$, and ZnONPs at different time intervals

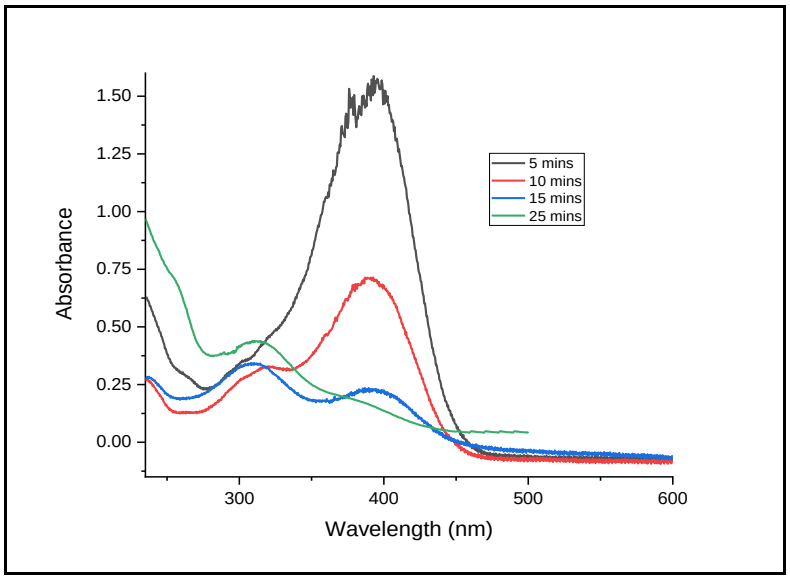

Figure 11. Absorption spectra of a reaction mixture containing 4-NP, $NaBH_4$, and ZnONPs@Cu-BTSC at different time intervals

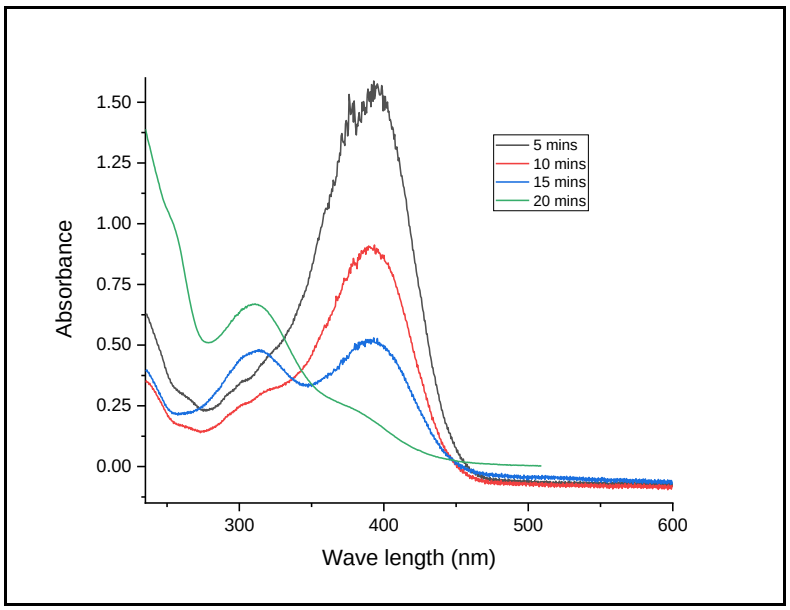

Figure 12. Absorption spectra of reaction mixture containing 4-NP, $NaBH_4$, and ZnONPs@Pd-BTSC at different time interval

The complete disappearance of peak at 400 nm takes 30 min for ZnONPs and whereas for ZnONPs@Cu-BTSC and ZnONPs@Pd-BTSC takes 25 and 20 minutes, respectively. The rate constants for ZnONPs, ZnONPs@Cu-BTSC, and ZnONPs@Pd-BTSC are 4.02×10^{-2}, 4.18×10^{-2}, and 4.54×10^{-2} min^{-1}, respectively.

Conclusions

As-synthesized zinc oxide nanoparticles (ZnONPs) and its post-functionalized ZnONPs@Cu-BTSC and ZnONPs@Pd-BTSC were synthesized and characterized based on UV-Visible and FT-IR spectroscopies, Powder X-

ray diffraction (PXRD) and Scanning electron microscopy-energy dispersive spectroscopy (SEM-EDS). The ZnONPs@Cu-BTSC and ZnONPs@Pd-BTSC were prepared by post-functionalization with copper and palladium complexes of 4-hydroxybenzaldehyde thiosemicarbazone(BTSC) ligand. The ligand and its Cu and Pd complexes were characterized based on mass spectral analysis. The grain size of zinc nanoparticles was determined using PXRD and SEM-EDX data. Surface functionalization of as-synthesized ZnONPs was evidenced by IR spectral analysis. The catalytic activity of ZnONPs, ZnONPs@Cu-BTSC, and ZnONPs@Pd-BTSC in reducing 4-nitrophenol to 4-aminophenol was investigated and compared. The ZnONPs@Pd-BTSC showed higher catalytic activity than ZnONPs@Cu-BTSC. Zinc oxide nanoparticles post-functionalized with metal complexes are reported by us for the first time. In several reports [36, 37], *in situ* generated (means without isolation), nanoparticles were used in the catalytic reactions. In the present study, ZnONPs, ZnONPs@Cu-BTSC, and ZnONPs@Pd-BTSC are isolated and used in catalytic reduction of 4-nitrophenol to 4-aminophenol.

Acknowledgments

Hussain Reddy is thankful to UGC for the award of the UGC-BSR Faculty Fellowship (Grant No.F.18-1/2011 (BSR).

Disclosure Statement

No potential conflict of interest was reported by the authors.

Orcid

Varun Kumar Bale 0000-0001-8256-9505

Hussain Reddy Katreddi 0000-0001-5543-7478

Supporting Information

Additional supporting information related to this article can be found, in the online version, at 10.26655/AJNANOMAT.2022.2.8

References

[1]. Rai M., Yadav A., Gade A. *Biotechnol Adv.*, 2009, **27**:76 [Crossref], [Google Scholar], [Publisher]

[2]. Sawai J. *J Microbiol Methods.*, 2003, **54**:177 [Crossref], [Google Scholar], [Publisher]

[3]. Hussain Reddy K. *Bioinorganic Chemistry;* New Age International: New Delhi, 2020, 102

[4]. Ozgur U., Ya I.A., Liu C., Teke A., Reshchikov M.A., Dogan S., Avrutin V., Cho S.J., Morkoc H. *J. Appl. Phys.*, 2005, **98**:041301 [Crossref], [Google Scholar], [Publisher]

[5]. Klingshirn C. *Phys Status Solidi(b).*, 2007, **244**:3027 [Crossref], [Google Scholar], [Publisher]

[6]. Wang A., Quan W., Zhang H., Li H., Yang S. *RSC Adv.*, 2021, **11**:20465 [Crossref], [Google Scholar], [Publisher]

[7]. Farahmandjou M., Khalili P. *Asian Journal of Green Chemistry*, 2021, **5**:219 [Crossref], [Google Scholar], [Publisher]

[8]. Rezaei-Aghdam E., Ali S., Khodadadi-Moghaddam M., Sahar M. *Asian Journal of Nanoscience and Materials*, 2021, **4**:188 [Crossref], [Publisher]

[9]. Anbuvannan M., Ramesh M., Manikandan E. *Asian Journal of Green Chemistry*, 2019, **3**:418 [Crossref], [Google Scholar], [Publisher]

[10]. Marzieh N., Ghazaleh K. *Asian J. Nanosci. Mater.*, 2021, **4**:290 [Crossref], [Publisher]

[11]. Siti N.S.J., Abdul H.A. *Asian Journal of Green Chemistry*, 2019, **3**:271 [Crossref], [Google Scholar], [Publisher]

[12]. Dey K., Paul S.,Ghosh P. *Asian J. Nanosci. Mater.*, 2021, **4**:159 [Crossref], [Google Scholar], [Publisher]

[13]. Parvin G., Amir M. *Asian J. Nanosci. Mater*., 2018, **2**:27 [Crossref], [Google Scholar], [Publisher]
[14]. Moghaddam F.M., Saeidian H., Mirjafary Z., Sadeghi A. *Journal of the Iranian Chemical Society,* 2009, **6**:317 [Crossref], [Google Scholar], [Publisher]
[15]. Tamaddon F., Amrollahi M.A., Sharafat L.A. *Tetrahedron Lett.*, 2005, **46**:7841 [Crossref], [Google Scholar], [Publisher]
[16]. Kumar B.V., Naik H.S.B., Girija D., Kumar B.V. *Journal of Chemical Sciences,* 2011, **123**:615 [Crossref], [Google Scholar], [Publisher]
[17]. Hosseini-Sarvari M. *Journal of the Iranian Chemical Society,* 2011, **8:**S119 [Crossref], [Google Scholar], [Publisher]
[18]. Yavari I., Beheshti S. *Journal of the Iranian Chemical Society,* 2011, **8:**1030 [Crossref], [Google Scholar], [Publisher]
[19]. Alinezhad H., Salehian F., Biparva P. *Synthetic Communications.*, 2012, **42:**102 [Crossref], [Google Scholar], [Publisher]
[20]. Grasset F., Saito N., Li D., Duguet E. *Journal of Alloys and Compounds*., 2003, **360**:298 [Crossref], [Google Scholar], [Publisher]
[21]. Mohankandhasamy R., Minakshi D., Seong Soo A. An-Dong Kee Y. *International Journal of Nanomedicine.*, 2014, **9**:3707 [Crossref], [Google Scholar], [Publisher]
[22]. Franziska K., Julian R., Julia M., Andreas H., Tobias V., Horst W., Silvia G., Wolfgang M. *Beilstein J. Org. Chem.*, 2015, **11**:678 [Crossref], [Google Scholar], [Publisher]
[23]. Nurun N.R., Jannatul M., Hashi A., Islam M.S., Hossain M.A., Elias M., Alam M.M., Karim M.R., Hasnat M.A., Nizamuddin M., Iqbal A.S. *International Journal of Chemical Reactor Engineering.*, 2016, **14**:785 [Crossref], [Google Scholar], [Publisher]
[24]. Khan A., Ullah M., Humayun M., Shah N., Chang B.P, Yaseen M. *Journal of Dispersion Science and Technology*., 2022, **43**:259 [Crossref], [Google Scholar], [Publisher]
[25]. Fouladi-Fard R., Aali R., Mohammadi-Aghdam S., Mortazavi-derazkola S. *Arabian Journal of Chemistry*., 2022, **15**:103658 [Crossref], [Google Scholar], [Publisher]
[26]. Wang Z., Ye X., Chen L., Huang P., Wang Q., Ma L., Hua N., Liu X., Xiao X., Chen S. *Mater. Sci. Semicond. Process*., 2021, **121**:105354 [Crossref], [Google Scholar], [Publisher]
[27]. Pandiyan N., Murugesan B., Arumugam M., Sonamuthu J., Samayanan S., Mahalingam S. *J. Photochem. Photobiol., B.*, 2019, **198**:111559 [Crossref], [Google Scholar], [Publisher]
[28]. Guo M., He J., Li Y., Ma S., Sun X. *J Hazard Mater*., 2016, **310**:89 [Crossref], [Google Scholar], [Publisher]
[29]. Wang L., Yang Q., Cui Y., Gao D., Kang J., Sun H., Zhu L., Chen S. *New J Chem*., 2017, **41**:8399 [Crossref], [Google Scholar], [Publisher]
[30]. Zhang J., Chen G., Guay D., Chaker M., Ma D. *Nanoscale.*, 2014, **6**:2125 [Crossref], [Google Scholar], [Publisher]
[31]. Varun Kumar B., Hussain Reddy K. *International Journal of Nano Dimensions*., 2022, **13**:214 [Crossref], [Google Scholar], [Publisher]
[32]. Varun Kumar B., Hussain Reddy K. *Journal of Advanced Scientific Research,* 2021, **12:**130 [Crossref], [Google Scholar], [Publisher]
[33]. Champion Y., Bigot J. *Mater Sci Eng.* A., 1996, **217-218**:58 [Crossref], [Google Scholar], [Publisher]
[34]. Giradin D., Maurer M. *Mat. Res. Bull*., 1990, **25**:119 [Crossref], [Google Scholar], [Publisher]
[35]. Boulaud D., Chouard J.C., Briand A., Chartier F., Lacour L., Mauchien P., Mermet J.M. *J. Aerosol Sci.,* 1992, **23**:S225 [Crossref], [Google Scholar], [Publisher]
[36]. Pangkita D., Ramesh C.D., Pankaj B. *New J. Chem.,* 2014, **38**:1789 [Crossref], [Google Scholar], [Publisher]
[37]. Kastner C., Thunemann A.F. *Langmuir*., 2016, **32**:7383 [Crossref], [Google Scholar], [Publisher]

How to cite this manuscript: Varun Kumar Bale, Hussain Reddy Katreddi*, Synthesis, characterization and catalytic activity of zinc oxide nanoparticles functionalized with metallo-thoiosemicarbazones. *Journal of Medicinal and Nanomaterials Chemistry*, 4(2) 2022, 159-173. DOI: 10.48309/JMNC.2022.2.7